Fuel Processing Technology 189 (2019) 74–79

Contents lists available at ScienceDirect

Fuel Processing Technology

journal homepage: www.elsevier.com/locate/fuproc

Research article

De-intercalation of the intercalated potassium in the preparation of activated carbons by KOH activation

Wenwen Wang, Shaoping Xu*, Kechao Wang, Jia Liang, Wei Zhang

State Key Laboratory of Fine Chemicals, Institute of Coal Chemical Engineering, School of Chemical Engineering, Dalian University of Technology, No. 2 Linggong Road, Dalian 116024, China

ARTICLE INFO

Keywords:
Activated carbon
Potassium
De-intercalation
Pore structure
Surface properties

ABSTRACT

In this study, the potassium formed during the activation of petroleum coke with KOH as activation agent was quantified, and three de-intercalation reagents (acetic acid, water vapor, methanol) with different flow and at different temperature were used to de-intercalate the potassium. It is suggested that the activation process yields almost the same amount potassium in the free state as that in the potassium-graphite intercalation compounds. The results also indicated that the introduction of acetic acid (250 °C, 0 .4ml/min), water vapor (200 °C, 0 .4ml/min), methanol (150 °C, 0 .4ml/min) could furthest improve the porosity and decrease the microcrystalline size as well as increase graphite layer spacing d_{002}. Moreover, the de-intercalation reagents could accelerate the formation of oxygen-containing groups on the surface of the activated carbons. Based on these results, the de-intercalation mechanism has been proposed.

1. Introduction

High specific surface area activated carbons (HSAAC) are promising materials as adsorbents for gas and liquid adsorption, as catalysts or catalyst supports for catalysis, and as electrodes of electrochemical capacitors and rechargeable batteries for energy storage [1–6]. The major route to produce HSAAC is the activation of various high carbonaceous raw materials such as petroleum coke and anthracite with KOH.

The activation mechanisms by KOH have been widely studied. Yamashita and Ouchi [7] studied the reaction mechanism of phenolic resin and alkali hydroxides. They proved that KOH could react with 'active hydrogen' sites including $–CH_2–$ and –CH– species to form potassium compounds (K_2CO_3 and K_2O), and a considerable amount of potassium was formed due to the reaction of potassium compounds and carbon at high temperature. Otowa T [8] investigated the adsorption capacity of HSAAC prepared by KOH activation and believed that potassium was formed from the potassium hydroxide by dehydration and reduction by hydrogen or carbon. Lillo-Rodenas et al. [9,10] calculated the standard Gibbs free energy of possible reactions during the chemical activation of Spanish anthracite, and proposed an overall activation mechanism that KOH could react with carbon to form metallic potassium, hydrogen and potassium carbonate. Raymundo-pinero et al. [11] studied the KOH activation mechanism of multiwalled carbon nanotubes. They found that KOH, K_2CO_3 and K_2O all could react with carbon at low temperature, but at high temperature, the only remained potassium species is K_2O, and potassium was finally formed from the reaction between K_2O and carbon. In our previous studies [12,13], the effects of K_2O and K_2CO_3 on the gas evolution during the KOH activation of petroleum coke were systematically studied. The –CH– and $–CH_2–$ species have been regarded as 'active carbon' sites during the KOH activation process. We also demonstrated that potassium compounds could react with the 'active carbon' sites to form metallic potassium, and the formation of potassium could enhance the activation reaction. Furthermore, we investigated the effects of hydrogen in the activation process, and found that the introduction of hydrogen could increase the quantity of 'active carbon' sites, which is favorable to the development of the porous structure of activated carbons (ACs).

As indicated above, during the activation with KOH, metallic potassium is inevitably formed. The potassium might intercalate in between the hexagonal carbon layers of the crystallite of ACs and so that plays an important role in porosity development [14–17]. Marsh [14] investigated the structural changes of the carbonaceous feedstock during KOH activation process, and considered that the intercalation of potassium would force apart the lamellae of the crystallite of the ACs. Xue et al. [15] used XRD to study the change in carbon structure in KOH activation. They found that there existed potassium-graphite intercalation compounds (K-GICs) in unwashed mesocarbon microbeads,

* Corresponding author.
E-mail address: huizixu@hotmail.com (S. Xu).

https://doi.org/10.1016/j.fuproc.2019.03.001
Received 25 December 2018; Received in revised form 25 February 2019; Accepted 4 March 2019

and the intercalation widened pores to form mesoporous structure. Raymundo-pinero et al. [11] analyzed the microcrystalline structure of carbon nanotubes with XRD. They found that the d_{002} increased from 0.35 nm to 0.40 nm and proved that the intercalation of potassium could promote the development of the porous structure of ACs.

Not only the intercalation of potassium but also the de-intercalation of K-GICs make contributions to the porosity development of ACs [18–20]. Romanos [18] found that metallic potassium could intercalate into graphitic layers and stretch the lattice, and the removal of intercalated potassium by oxygen could result in the expansion of pore network that corresponds to an increase in porosity. Won-Chun Oh et al. [19] synthesized K-GICs by the modified two-bulb method and kept the samples in the air for several weeks, the analysis of XRD indicated that there was a de-intercalation process that could expand the distance of the graphitic microcrystalline of the ACs. They also considered two kinds of stage transformation—statistical de-intercalation and irregular de-intercalation of graphite de-intercalation compounds with disordered stages.

As above-mentioned, the de-intercalation of potassium would possibly be able to improve the porosity development and provide convenience for doping of ACs, and so that to modify the properties of ACs to match different applications. Furthermore, it makes more effective use of the potassium produced during KOH activation and makes the activation process safer. In this study, ACs were prepared from petroleum coke with KOH as activation agent. The potassium formed during the activation process was quantified. CH_3COOH , H_2O , CH_3OH were chosen as de-intercalation reagents to react with the K-GICs formed during the activation. The porosity development and surface properties of the resultant ACs prepared by de-intercalation with three O-containing reagents at different temperature and reagent flow were investigated by using BET, FTIR, Boehm titration, XRD and XPS analysis to provide an insight into the mechanism of de-intercalation.

2. Experimental

2.1. Preparation of ACs

Petroleum coke from Liaoyang Petrochemical Company was used as precursor of the ACs. It was ground and sieved to the particle size range of 0-150 μm. The proximate and ultimate analysis of the petroleum coke is listed in Table 1.

4 .5g of the petroleum coke was mixed with13.5g KOH, 13.5ml H_2O and 1.35 ml CH_3CH_2OH at room temperature. As shown in Fig. 1, under a nitrogen flow of 70 ml/min, the mixture was electrically heated in a laboratory tube reactor with a rate of 8 °C /min from room temperature to 800 °C, holding at 800 °C for 1 h, and cooling down to a desired temperature. At this temperature, the de-intercalation reagent would transfer from liquid to gas through a heating furnace and then entrained in nitrogen flow into the reactor. When the de-intercalation reaction completed, which was indicated by the ending of the H_2 evolution as discussed below, the reactor was cooled down to room temperature. The sample obtained was washed with distilled water until the filtrate became neutral to obtain the products. The AC prepared under N_2 atmosphere without de-intercalation was donated as AC-N_2, the AC de-intercalated with different reagent at different temperature and reagent flow was donated as AC-R-T-F (R: reagent, T: temperature in °C, F: reagent flow in ml/min).

During the de-intercalation process, the evolved gas mixture was analyzed by a GC-920 chromatography (column: packed 5A molecular sieves, 40 °C; detector: thermal conductivity detector, 70 °C; carrier gas: argon, flow rate: 18cm^3/min). The analysis data was recorded by a NC-2000 chromatograph data workstation.

2.2. Characterization of ACs

The porous textures of ACs were deduced from the adsorption isotherms of N_2 at 77 K measured by a BWJK122W apparatus. The specific surface areas were calculated using the Brunauer-Emmett-Teller (BET) equation. The total volumes were estimated from the liquid volume of nitrogen adsorbed at relative pressure $p/p_0 = 0.98$. The micropore volumes were calculated by constructing the t-plots. The micropore and mesopore size distributions were obtained by the Horvath-Kawazoe (H—K) method and Barret-Joyner-Halenda (BJH) method, respectively.

Fourier transform infrared spectrometer (Nicolet-20DXB, Thermo Nicolet Nexus) was used to detect the surface functional groups in the wave-number range of 500–4000 cm^{-1}.

The surface oxygen-containing groups, i.e. the carboxyl, phenolic hydroxyl, lactone and carbonyl groups, were quantitatively measured by Boehm titration [21].

X-ray diffraction analysis (XRD) (D/Max2400, RIGAKU) with Cu Kα X-rays (λ = 0.154 nm) and Ni filter from 5°to 80°(2θ) with a step of 0.02° was conducted to analyze the crystal structure of ACs.

X-ray photoelectron spectroscopy (XPS) analysis were carried out using a ThermoFisher X-ray photoelectron spectrometer (ESCALAB™ 250Xi) equipped with a dual beam charge neutralizer.

3. Results and discussion

3.1. The quantitative evaluation of potassium formed during the activation

Potassium formed during the activation with KOH could be intercalated, i.e. in the state of K-GICs, or be free on the surface of the reactor wall. Both kinds of potassium are highly reactive. Therefore, a controlled introduction of the de-intercalation reagent could modify the ACs through the reaction of the reagent with the K-GICs. A mild consumption of the free potassium through the reaction of the reagent with it could make the process safe as well.

To make a quantitative evaluation of the distribution of potassium in K-GICs or in free state, a two-step de-intercalation experiment has been designed: all the selected de-intercalation reagents should react with potassium to produce H_2 gas, so that these de-intercalation reactions could be followed by monitoring the reaction gases evolved. The quantity of potassium could be calculated through the content of H_2. During the de-intercalation process, a stream of 0 .4ml/min alcohol with a large dynamic molecular was introduced at 250 °C into the reaction system firstly. The dynamic molecular size of the alcohol should be larger than that of the distance between the graphitic layers expanded by the intercalated potassium in K-GICs. Therefore, the alcohol would react only with the potassium in free state. After the reaction involved with the alcohol is completed, the above three de-intercalation reagent with a stream of 0 .4ml/min could be introduced into the reaction system at 250 °C, for they are with much smaller molecular size,

Table 1
Proximate and ultimate analysis of petroleum coke.

Proximate analysis (wt%, ad.)				Ultimate analysis (wt%, daf.)				
Ash	Moisture	Volatile	Fixed carbon	Carbon	Hydrogen	Oxygen[a]	Nitrogen	Sulfur
0.64	4.90	17.41	77.05	88.35	3.87	4.24	2.95	0.59

[a] By difference.

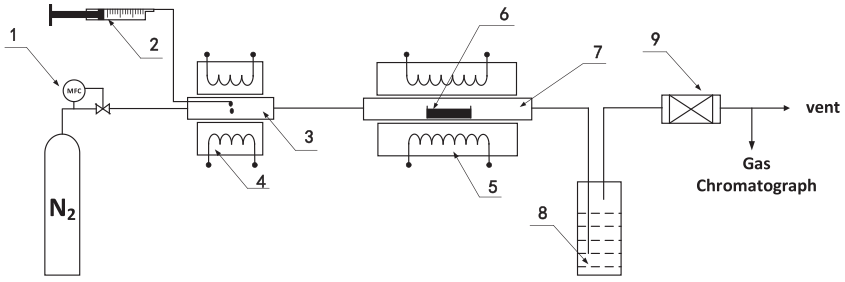

Fig. 1. Schematic diagram of preparation of ACs.
1. Mass flow controller; 2. Pump; 3. Gasifier; 4,5. Furnace; 6. KOH/coke mixture in boat; 7. Pipe reactor: 8. Scrubbing bottle; 9. Dryer.

Table 2
Distribution of potassium quantified with different alcohol and water (mmol).

	Butanol + H_2O	Hexyl alcohol + H_2O	Heptanol + H_2O
K in free state	4.49	3.01	3.10
K-GICs	1.21	2.46	2.44
Total	5.70	5.47	5.54

the potassium in K-GICs is reachable.

First, the kind of alcohol should be confirmed. As the method stated above, the evolved gas mixture produced by alcohol and potassium in free state, H_2O and potassium in K-GICs were gathered by drainage gas gathering method, respectively. The quantity of potassium was calculated by drainage volume and the volume content of H_2.

As shown in Table 2, the total amount of potassium is almost the same quantified with different alcohol and water. While compared the result with butanol and hexyl alcohol, the difference of the potassium distribution means that the dynamic molecular of butanol is not suitable for part of K-GICs could react with it. When further increase the molecular size of alcohol, as in the case for hexyl alcohol and heptanol, the potassium distribution is nearly invariable. It means that hexyl alcohol is big enough and could react with only the potassium in free state, but not those intercalated. Therefore, hexyl alcohol is selected as the de-intercalation reagent in the first step.

The variation of H_2 content in the evolved gas with time on stream during the de-intercalation is shown in Fig. 2. H_2 evolution begins upon the introduction of hexyl alcohol. After 36 min, there is no more H_2, which indicates the potassium in free state have been all reacted. At this point, when the de-intercalation reagent with small dynamic diameter is introduced, a considerable amount of H_2 is again formed, which indicates that the K-GICs have been reacted with the de-intercalation reagents. The time when the maximum H_2 evolution reaches and the reaction time duration vary with the de-intercalation reagent in the order of acetic acid < water < methanol. Nevertheless, the amounts of H_2 that formed in the de-intercalation process are almost the same for the three de-intercalation reagents. Accordingly, the reactivity of the de-intercalation reagent depends mainly on its acidity and is possibly irrelevant to its molecular size.

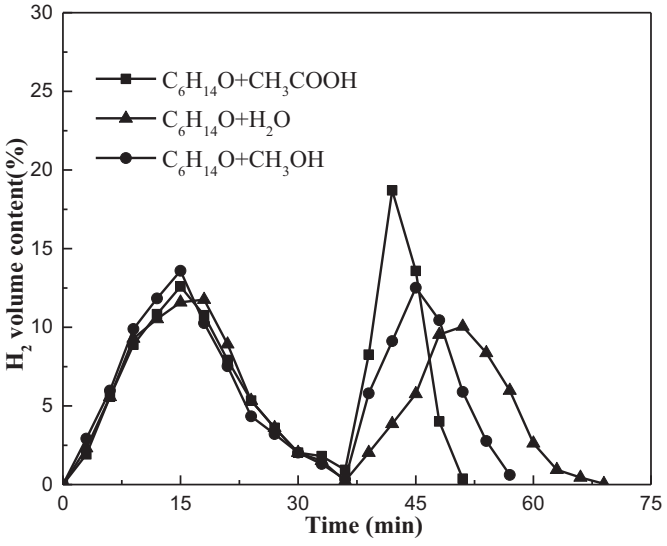

Fig. 2. Variation of H_2 content in the evolved gas with time on stream during the de-intercalation.

Still, Fig. 2 shows that H_2 evolution peak areas formed by the de-intercalation with hexyl alcohol are approximately the same as that with the other de-intercalation reagents. It is suggested that the activation process yields almost the same amount potassium in the free state as that in the K-GICs. The value of the number of potassium to that of carbon in the K-GIC is far from the saturated one known as in KC_8. It is therefore necessary to find a way to increase the intercalation ratio or take advantage of the potassium in free state, so that to enhance the efficiency and safety of the preparation process.

3.2. Porosity development during the de-intercalation

The porosity development of ACs in regards of BET surface area and pore volume were investigated by varying the de-intercalation temperature and de-intercalation reagent flow.

Table 3 shows the porous structure parameters of the ACs obtained by introducing the de-intercalation reagents of constant flow 0 .4ml/min at different de-intercalation temperature. With the increase of de-intercalation temperature, the porous structures of the ACs in regards of specific surface area and pore volume increased at the lower temperature range, and then decreased at the higher temperature. For a specific de-intercalation reagent, there was a moderate temperature under

Table 3
Porous structure parameters of ACs prepared at different de-intercalation temperature.

Sample	Temperature(°C)	$S_{BET}(m^2/g)$	$V_t(cm^3/g)$	$V_{micro}(cm^3/g)$
AC-N_2	–	2430	1.25	1.10
AC-CH_3COOH	100	2209	1.86	0.96
	150	2410	1.97	1.01
	200	2721	2.02	1.13
	250	2799	2.28	1.21
	300	2205	1.86	0.96
AC-H_2O	100	2731	2.01	1.15
	150	2671	2.10	1.12
	200	2923	2.19	1.26
	250	2728	1.96	1.16
	300	2362	1.25	1.04
AC-CH_3OH	100	2197	1.95	0.93
	150	2871	2.01	1.18
	200	2731	1.94	1.15
	250	2591	2.20	1.09
	300	2530	2.11	1.06

Table 4
Porous structure parameters of ACs prepared under different de-intercalation reagent flow.

Sample	Temperature(°C)	Regent flow (ml/min)	$S_{BET}(m^2/g)$	$V_t(cm^3/g)$	$V_{micro}(cm^3/g)$
AC-N_2	–	–	2430	1.25	1.10
AC- CH_3COOH	250	0.2	2562	2.04	1.09
		0.4	2799	2.28	1.21
		0.6	2709	2.14	1.14
		0.8	2502	2.00	1.07
		1.0	2188	1.85	0.90
AC-H_2O	200	0.2	2259	1.76	0.93
		0.4	2923	2.19	1.26
		0.6	2759	2.40	1.11
		0.8	2708	2.12	1.19
		1.0	2531	2.03	1.08
AC-CH_3OH	150	0.2	1994	1.76	0.74
		0.4	2871	2.01	1.18
		0.6	2145	1.82	0.88
		0.8	2069	1.80	0.88
		1.0	1976	1.76	0.73

which the porosity development of AC was favorated. The favorate temperature varied with different de-intercalation reagent, and it was around 250 °C, 200 °C and150 °C for CH_3COOH, H_2O and CH_3OH, respectively. With CH_3COOH, H_2O and CH_3OH as de-intercalation reagents, the porosity developments were not limited to those micropores.

As shown in Table 4, the effect of de-intercalation reagent flow on the porosity development of ACs was similar to that of the de-intercalation temperature. With the increase of the de-intercalation reagent flow, the specific surface area and the pore volume of ACs increased firstly and then decreased. The optimal flow for the de-intercalation reagents was 0 .4ml/min.

3.3. O-containing surface groups introduced by the de-intercalation

The IR, Boehm titration and XPS analysis were used to investigate the O-containing surface groups of the ACs prepared at the optimal de-intercalation temperature and reagent flow, i.e. acetic acid (250 °C, 0 .4ml/min), water vapor (200 °C, 0 .4ml/min), methanol (150 °C, 0 .4ml/min).

Fig. 3 shows the FTIR spectra of the feedstock petroleum coke and the resultant ACs de-intercalated with different reagent. It can be seen that the kinds of the functional groups on the surface of the resultant ACs were nearly invariable compared with that of the feedstock petroleum coke. The IR bands at around 3400 cm^{-1} is assigned to O—H stretching vibration mode of hydroxyl functional groups. The band around 3050 cm^{-1} could be the stretching mode of aromatic unsaturated hydrocarbon groups. The bands around 2920 cm^{-1} and 2850 cm^{-1} are associated with C—H stretching vibrations in aliphatic such as $–CH_2$, $–CH_3$ and $–CH_2CH_3$. The band around 1600 cm^{-1} and 1440 cm^{-1} are asymmetric and symmetric C═C deformation vibrations because of the conjugation with another C═C and C—O of benzene ring. The broad band at approximately 1200 cm^{-1} may be due to O—H bending modes and the overlapping of C–O–C stretching, C—O stretching and bending modes of alcoholic, phenolic and carboxylic groups.

The results of Boehm titration are represented in Table 5. The introduction of the three O-containing de-intercalation reagents could make the content of carboxyl and phenolic hydroxyl increased, while the content of carbonyl decreased. Though the original sample is treated by the method of water washing, the amounts of O-containing functional groups are less than that of H_2O-200-0.4, which is because appropriate temperature and reagent flow offered during the de-intercalation process support the de-intercalation minienvironment, and be in favor of the formation of functional groups.

Table 6 summarizes the relative area of C1s XPS. It can be seen that graphitic or aromatic carbon (284.4eV) are the most predominant

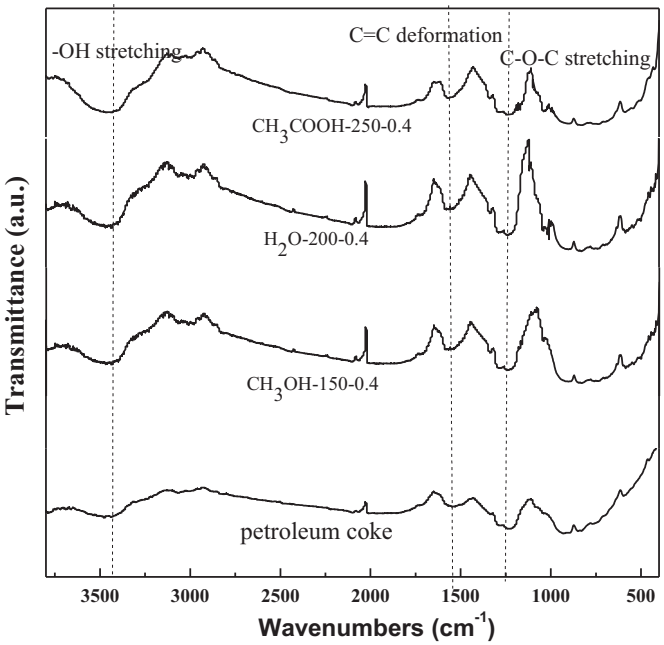

Fig. 3. FTIR spectra of the raw material and ACs prepared with different de-intercalation reagent.

Table 5
Boehm titration analysis of the ACs (mmol/g).

Sample	Carboxyl	Lactone	Phenolic hydroxyl	Carbonyl
Petroleum coke	0.33	–	0.22	0.56
AC-N_2	0.37		0.39	0.50
CH_3COOH-250-0.4	0.62	–	0.46	0.49
H_2O-200-0.4	0.61	–	0.49	0.33
CH_3OH-150-0.4	0.42	–	0.53	0.31

functional groups on the surface of the ACs. The introduction of CH_3COOH and H_2O could more likely to increase the percentages of carboxyl (288.6 eV), and the introduction of CH_3OH would form more hydroxyl, ethers and C═N groups (285.7 eV) [22]. The results are consistent with the Boehm titration.

3.4. Microcrystalline structure changes during the de-intercalation

Fig. 4 illustrates the XRD patterns of the ACs. It can be clearly seen that there are two broad diffraction peaks around $2\theta = 25°$ and

Table 6
Relative area (%) of C1s XPS.

Sample	Graphitic, aromatic (284.4eV)	Hydroxyl, ethers, C=N groups (285.7eV)	Carbonyl (286.9eV)	Carboxyl (288.6eV)
AC-N_2	52.4	19.3	15.4	12.9
CH_3COOH-250-0.4	44.0	23.0	15.2	17.8
H_2O-250-0.4	46.6	21.1	15.9	16.4
CH_3OH-150-0.4	46.8	27.8	15.0	10.4

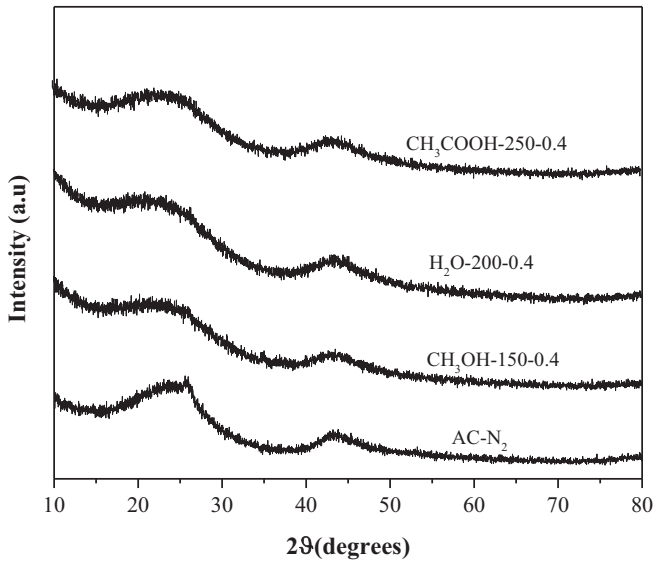

Fig. 4. XRD patterns of the ACs prepared with different de-intercalation reagent.

Table 7
Microcrystalline structural parameters of the ACs with different de-intercalation reagent.

Sample	2θ (°)	d_{002} (nm)	L_c (nm)	L_a (nm)
AC-N_2	24.385	0.365	1.05	2.68
CH_3COOH-250-0.4	23.207	0.383	0.88	2.11
H_2O-200-0.4	23.326	0.381	0.89	2.29
CH_3OH-150-0.4	22.489	0.374	0.95	2.26

2θ = 43° in each spectrum, corresponding to the diffraction of (002) and (100), respectively. The broad 002 peak corresponding to the interlayer distance of the original materials shifts to a higher value. Compared with original sample, the two peaks of the ACs de-intercalated with reagents are broader but their intensity drops, it indicates that the introduction of de-intercalation reagents makes the graphite disordered and the graphite layer spacing d_{002} increased.

Microcrystalline structural parameters of the petroleum coke and its activated samples are shown in Table 7. The size of the graphitic microcrystalline is determined by Lc and La. Compared with original sample, Lc and La of the ACs de-intercalated with the three O-containing de-intercalation reagents decreased and d_{002} increased. It indicated that the de-intercalation of K-GICs made the crystallite size decreased, and expanded the distance of hexagonal carbon layers of the crystallite, which promoted the porosity development.

Based on the above results, the mechanism of de-intercalation with O-containing reagents was proposed. During the activation process, KOH could react with carbon or –CH-、$-CH_2-$ to from a considerable amount of potassium. Part of the metallic potassium intercalates into the layer of graphite, and expands the distance of hexagonal carbon layers of the crystallite. The intercalated potassium is active and can further react with the three O-containing de-intercalation reagents, combined with different kinds of molecular structure derived from the de-intercalation reagent to bring more O atom to the ACs, and release H_2 at the same time. At last, the activated sample will be washed with acid and distilled water, the potassium compounds and other impurities are removed, the distance of hexagonal carbon layers of the crystallite will be further expanded, then the product is obtained. De-intercalation with the O-containing reagents could improve the pore structure of activated carbon, and introduce higher content of O-containing functional groups to activated carbon.

4. Conclusions

De-intercalation of potassium formed during KOH activation process has been conducted using three O-containing de-intercalation reagents in this paper.

Two-step de-intercalation method was adopted to make a quantitative evaluation of potassium. The introduction of two de-intercalation reagents with different molecular size could react with potassium in free state and in K-GICs, respectively. It is suggested that the activation process yields almost the same amount potassium in the free state as that in the K-GICs.

The microenvironment of de-intercalation process at appropriate reaction conditions is more conductive to modify the properties of ACs. The introduction of the three O-containing de-intercalation reagents could react with potassium and other functional groups. De-intercalation process could promote the formation of the pore structure and bring some O-containing functional groups to the surface of ACs, the porosity structure and surface properties of ACs have been developed greatly.

Microcrystalline structure is also affected during the de-intercalation process. The removal of potassium expands the distance of hexagonal carbon layers of the crystallite, makes the crystallite size decreased and the graphite disordered.

De-intercalation is a novel and promising method to control and modify the properties of ACs to match different applications. We will discuss more of the de-intercalation process, give an insight into the de-intercalation mechanism and integrate experiment with application in the next stage.

Acknowledgments

This work was supported by the National Natural Science Foundation of China (No.21376046).

References

[1] Elena Rodríguez, Roberto García, Low-cost hierarchical micro/macroporous carbon foams as efficient sorbents for CO_2 capture [J], Fuel Process. Technol. 156 (2017) 235–245.
[2] J. Romanos, T. Rash, S. Abou Dargham, et al., Cycling and regeneration of adsorbed natural gas in microporous materials[J], Energy & Fuels 31 (12) (2017) 14332–14337.
[3] L. Fuhu, C. Weidong, S. Zengmin, et al., Activation of mesocarbon microbeads with different textures and their application for supercapacitor[J], Fuel Process. Technol. 91 (1) (2010) 17–24.
[4] M. Sevilla, R. Mokaya, Energy storage applications of activated carbons: supercapacitors and hydrogen storage, Energy Environ. Sci. 7 (4) (2014) 1250–1280.
[5] A. Gabe, R. Ruiz-Rosas, D. Cazorla-Amorós, et al., Modeling of oxygen reduction reaction in porous carbon materials in alkaline medium. Effect of microporosity, J. Power Sources 412 (2019) 451–464.

[6] Tanya Tsoncheva, Genova, et al. transition metal modified activated carbons from biomass and coal; treatment products as catalysts for methanol decomposition [J], Reaction Kinetics Mechanisms & Catalysis 110 (2) (2013) 281–294.
[7] Y. Yamashita, K. Ouchi, Influence of alkali on the carbonization process—I: carbonization of 3, 5-dimethylphenol-formaldehyde resin with NaOH, Carbon. 20 (1) (1982) 41–45.
[8] T. Otowa, R. Tanibata, M. Itoh, Production and adsorption characteristics of MAXSORB: high-surface-area active carbon, Gas Separation & Purification. 7 (4) (1993) 241–245.
[9] M.A. Lillo-Ródenas, D. Cazorla-Amorós, A. Linares-Solano, Understanding chemical reactions between carbons and NaOH and KOH [J], Carbon. 41 (2) (2003) 267–275.
[10] M.A. Lillo-Ródenas, J. Juan-Juan, D. Cazorla-Amorós, et al., About reactions occurring during chemical activation with hydroxides [J], Carbon. 42 (7) (2004) 1371–1375.
[11] E. Raymundo-Pinero, P. Azais, T. Cacciaguerra, et al., KOH and NaOH activation mechanisms of multiwalled carbon nanotubes with different structural organisation [J], Carbon. 43 (4) (2005) 786–795.
[12] C. Lu, S. Xu, C. Liu, The role of K_2CO_3 during the chemical activation of petroleum coke with KOH [J], Journal of Analytical & Applied Pyrolysis. 87 (2) (2010) 282–287.
[13] R. Xiao, S. Xu, Q. Li, et al., The effects of hydrogen on KOH activation of petroleum coke [J], Journal of Analytical & Applied Pyrolysis. 96 (2012) 120–125.
[14] H. Marsh, F. Rodríguez-Reinoso, Chapter 4 – characterization of activated carbon [J], Activated Carbon (2006) 143–242.
[15] R. Xue, Z. Shen, Formation of graphite-potassium intercalation compounds during activation of MCMB with KOH [J], Carbon. 41 (9) (2003) 1862–1864.
[16] Natalia García Asenjo, C. Botas Velasco, Clara Blanco Rodríguez, et al., Synthesis of activated carbons by chemical activation of new anthracene oil-based pitches and their optimization by response surface methodology[J], Fuel Process. Technol. 92 (10) (2011) 1987–1992.
[17] J. Wu, V. Montes, L.D. Virla, et al., Impacts of amount of chemical agent and addition of steam for activation of petroleum coke with KOH or NaOH[J], Fuel Process. Technol. 181 (2018) 53–60.
[18] J. Romanos, M. Beckner, T. Rash, et al., Nanospace engineering of KOH activated carbon[J], Nanotechnology. 23 (1) (2012) 015401.
[19] W.C. Oh, S.J. Cho, Y.S. Ko, The stability of potassium-graphite deintercalation compounds [J], Carbon. 34 (2) (1996) 209–215.
[20] N. Yoshizawa, K. Maruyama, Y. Yamada, et al., XRD evaluation of KOH activation process and influence of coal rank[J], Fuel. 81 (13) (2002) 1717–1722.
[21] H.P. Boehm, Surface oxides on carbon and their analysis: a critical assessment [J], Carbon. 40 (2) (2002) 145–149.
[22] N. Soudani, S. Najar-Souissi, V.K. Abderkader-Fernandez, et al., Effects of nitrogen plasma treatment on the surface characteristics of olive stone-based activated carbon[J], Environ. Technol. Lett. 38 (8) (2017) 11.